END
DATE
FILMED

10 83
DTIC

1.0

2.8 2.5

3.2 2.2

3.6

4.0 2.0

1.1

1.8

1.25 1.4 1.6
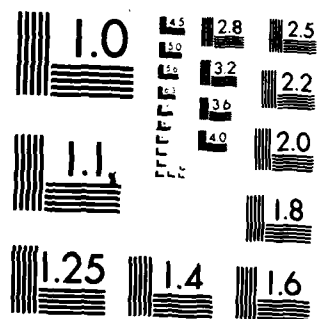
MICROCOPY RESOLUTION TEST CHART
NATIONAL BUREAU OF STANDARDS-1963-A

AD-A133209

Performance Characteristics of Passive Coherence Estimators

A. A. GERLACH

Systems Engineering and Advanced Concepts Branch
Acoustics Division

August 31, 1983

DTIC
ELECTE
SEP 2 9 1983

E

NAVAL RESEARCH LABORATORY
Washington, D.C.

83 09 28 025

REPORT DOCUMENTATION PAGE		READ INSTRUCTIONS BEFORE COMPLETING FORM
1. REPORT NUMBER NRL Report 8729	2. GOVT ACCESSION NO. AD-A133 207	3. RECIPIENT'S CATALOG NUMBER
4. TITLE *(and Subtitle)* PERFORMANCE CHARACTERISTICS OF PASSIVE COHERENCE ESTIMATORS		5. TYPE OF REPORT & PERIOD COVERED Interim report on a continuing NRL problem.
		6. PERFORMING ORG. REPORT NUMBER
7. AUTHOR(s) A. A. Gerlach		8. CONTRACT OR GRANT NUMBER(s) N00039-83WRDK039.4
9. PERFORMING ORGANIZATION NAME AND ADDRESS Naval Research Laboratory Washington, DC 20375		10. PROGRAM ELEMENT, PROJECT, TASK AREA & WORK UNIT NUMBERS 61153; XR01405-600; 51-1915-03
11. CONTROLLING OFFICE NAME AND ADDRESS Naval Electronic Systems Command Research and Technology Group Washington, DC 20360		12. REPORT DATE August 31, 1983
		13. NUMBER OF PAGES 25
14. MONITORING AGENCY NAME & ADDRESS(*If different from Controlling Office*)		15. SECURITY CLASS. *(of this report)* UNCLASSIFIED
		15a. DECLASSIFICATION/DOWNGRADING SCHEDULE

16. DISTRIBUTION STATEMENT *(of this Report)*

Approved for public release; distribution unlimited.

17. DISTRIBUTION STATEMENT *(of the abstract entered in Block 20, if different from Report)*

18. SUPPLEMENTARY NOTES

19. KEY WORDS *(Continue on reverse side if necessary and identify by block number)*

Coherence estimators
Detection performance
Signal processing

20. ABSTRACT *(Continue on reverse side if necessary and identify by block number)*

    Two-dimensional coherence processing is commonly used for passive detection in acoustic sensor systems. Modern coherence processors, well suited for this purpose, include the magnitude-squared coherence (MSC) estimator and the normalized correlation envelope (NCE) estimator. These are biased estimators, whose performance characteristics are not well understood and are exceptionally difficult to analyze. However, by developing a rather unique bias-correcting function, the detection performance of biased estimators is derived as a function of both the input-signal and the processor parameters. Design parameters, which optimize detection, are determined for both the MSC and the NCE estimators.

(Continues)

DD FORM 1473   EDITION OF 1 NOV 65 IS OBSOLETE
1 JAN 73

20. ABSTRACT (Continued)

In applications where the number of degrees of freedom (or time-bandwidth product) of a target signal is severely limited, detection performance can be enhanced by signal overcontainment within the processor bandwidth. Performance data are presented in formats appropriate for selecting processor parameters which are optimum for a given application. Practical guidelines are given to avoid misapplying the theoretical results in cases where there are many narrowband interfering signals in the spectral region of a target signal.

Accession For

NTIS GRA&I   X
DTIC TAB
Unannounced
Justification

By
Distribution/
Availability Codes
        Avail and/or
Dist   Special

A

CONTENTS

PERFORMANCE CHARACTERISTICS
OF PASSIVE COHERENCE ESTIMATORS

INTRODUCTION

Passive coherent processing is commonly used to detect a target signal present at two sensors remotely located in a transmission medium. Typically, the target signal at each sensor is contaminated by broadband noise, and the received signals are correlated over a two-dimensional ambiguity surface to compensate for time-register and doppler differences in the received target signal. Thresholding is employed to detect when and where (over the ambiguity surface) the correlator output exceeds a preset value. Performance measures for such a system include the detection versus false-alarm probabilities as a function of the input signal-to-noise ratios.

Modern coherence processors, which are well suited for passive detection, include the magnitude-squared coherence (MSC) estimator [1-3] and the normalized correlation envelope (NCE) estimator [4]. These processors are normalized and provide an output signal whose statistics, for uncorrelated signals, are essentially independent of the input signal levels. Thus, the false-alarm rate for a given threshold is effectively stabilized. For a given threshold (false-alarm probability), detection is optimum when the target signal energy required for detection is minimized.

Until recently, the general opinion of researchers was that detection was optimum when the processor bandwidth was matched to the spectral bandwidth of the target signal. There is good reason to suspect this to be true, since this condition maximizes the ratio of the mean-peak correlation output to the standard deviation of the output when the signals are uncorrelated [5]. Bandwidths greater than the signal bandwidth, moreover, increase the noise power without increasing the signal power. (Such a condition is termed "overcontainment" of the target signal and is employed to ensure containing the desired signal within the processor bandwidth when its bandwidth is unknown or highly nonstationary.) However, recent studies by Joseph LaPointe demonstrate that overcontainment can actually improve the detection sensitivity of the MSC estimator under certain conditions [6, 7]. These conditions occur when the number of degrees of freedom (or time-bandwidth product) of the target signal is less than a critical value, which depends on the input signal-to-noise ratios. In this report, detection performance is studied in a general context, and optimum design parameters are determined for both the NCE and the MSC estimators when they are employed as passive target-signature detectors.

SIGNAL DESCRIPTION AND REPRESENTATION

In a passive detection system, the processor input usually consists of signals from two remote sensors. In general, the signals from the two sensors are uncorrelated until the delay time and doppler difference of a common narrowband target signal $u(t)$ are properly compensated. After compensation, the two signal inputs may be expressed as

$$s_1(t) = a_1 u(t) + n_1(t) \tag{1a}$$

and

$$s_2(t) = a_2 u(t) + n_2(t), \tag{1b}$$

where $n_1(t)$ and $n_2(t)$ are the uncorrelated noise-background signals of the two channels. For purposes of this report, it is assumed that the power spectral density of the target signal $u(t)$ is uniformly distributed and confined within a narrow bandwidth of W Hz, the power spectral density of the noise signals is uniformly distributed over the processor bandwidth of B Hz, and the target signal is completely contained within B ($W \leqslant B$). The resultant power and crosspower of the two input signals are

$$\langle s_1^2(t) \rangle = (1 + r^2)\langle n_1^2(t) \rangle, \tag{2a}$$

$$\langle s_2^2(t) \rangle = (1 + r^2/\rho^2)\langle n_2^2(t) \rangle, \tag{2b}$$

and

$$\langle s_1(t)s_2(t) \rangle = \frac{r^2}{\rho} \sqrt{\langle n_1^2(t) \rangle \langle n_2^2(t) \rangle}, \tag{2c}$$

where

$$r^2 = a_1^2 \langle u^2(t) \rangle / \langle n_1^2(t) \rangle \tag{3a}$$

and

$$\rho^2 = a_1^2 \langle n_2^2(t) \rangle / a_2^2 \langle n_1^2(t) \rangle. \tag{3b}$$

In the above relations, r^2 is the input signal-to-noise power ratio of the one channel and ρ^2 is the ratio of the input signal-to-noise power ratios in the two channels. (This notation will prove convenient in the analysis to follow.)

Normalized Signal Correlation

The normalized correlation (or peak coherence) of the input signals is defined as the ratio of the peak signal crosspower to the geometric mean of the input signal power [4]. Thus, from Eq. (2), the normalized correlation of the signals $s_1(t)$ and $s_2(t)$ is

$$\gamma(r;\rho) = \frac{r^2}{\sqrt{(1 + r^2)(\rho^2 + r^2)}}. \tag{4}$$

The normalization bounds the peak coherence between the limits 0 and 1, regardless of the input signal levels, thus providing a measure of the correlation coefficient. The problem of thresholding for a given false-alarm rate is thereby greatly simplified.

Correlation Output Signal-to-Background Ratio

In the past, a measure of performance in detection processors has been the ratio of the mean-peak signal crosspower to the standard deviation of the signal crosspower when the signals are uncorrelated [5]. This measure is the correlation output signal-to-background ratio and is expressed as a function of the input signal-to-noise ratios. In the case under consideration, Eq. (2c) gives the mean-peak crosspower. The uncorrelated signal crosspower is evidenced over remote areas of the two-dimensional ambiguity surface where the time and/or doppler differences between the target signal inputs are uncompensated. In this area, the variance of the input signal crosspower may be shown to be [8]

$$
\sigma_o^2 = \frac{< n_1^2(t)> < n_2^2(t)>}{2BT\rho^2} \left[(1+r^2)(\rho^2 + r^2) + \left(\frac{B}{W} - 1\right) r^4 \right],
\tag{5}
$$

where T is the integration time of the correlation processor. Consequently, from Eqs. (2c) and (5), the mean-peak output signal-to-background ratio may be written as

$$
\frac{<s_1(t)s_2(t)>}{\sigma_o} = \frac{\sqrt{2BT}\; r^2}{\sqrt{(1+r^2)(\rho^2 + r^2) + \left(\frac{B}{W} - 1\right) r^4}}
$$

$$
= \frac{\sqrt{2BT}\; \gamma}{\sqrt{1 + \left(\frac{B}{W} - 1\right)\gamma^2}}.
\tag{6}
$$

The above ratio can vary only between the limits 0 and $\sqrt{2WT}$.

Effect of Processor Bandwidth B

The effect of the processor bandwidth B ($W \leq B$) on the above relations is not immediately apparent, since the input signal-to-noise power ratio r^2 is a function of B. To study the effect of the processor bandwidth, the variable r_o^2 is defined as the input signal-to-noise power spectral density ratio. Thus, $r^2 = r_o^2 / B$ and Eq. (6) becomes

$$
\frac{<s_1(t)s_2(t)>}{\sigma_o} = \frac{\sqrt{2T}\; r_o^2}{\sqrt{B\rho^2 + (1+\rho^2) r_o^2 + \frac{r_o^4}{W}}}.
\tag{7}
$$

It is obvious, then, that the mean-peak output signal-to-background ratio maximizes for B equal to W, except when ρ is zero. In this case, however, the correlation processor becomes a perfect matched filter (since the signal-to-noise ratio of the second input is infinity), and the noiseless signal input serves as an optimum (or matched) filter for the processor.

From the above analysis, it would appear that the optimum choice for the processor bandwidth would be to make it equal to the target signal bandwidth. However, the story is not yet complete. The crux of the optimization problem centers around minimizing the expected target signal energy required to equal or exceed the threshold for a given false-alarm probability. One

3

may readily perceive, from Eq. (5), that the variance of the unnormalized correlation output is nonstationary and varies with the power of the two input signals. Consequently, some form of normalization of the processor output is required if the false-alarm rate is to remain fixed for a given threshold level of the processor output. The following analysis is therefore directed to the performance of the class of normalized coherence estimators whose idealized performance is given in Eq. (4).

CORRELATION ESTIMATORS

The correlation estimators to be studied are the normalized correlation envelope (NCE) estimator and the magnitude-squared coherence (MSC) estimator. Both compute the ratio of the average signal crosspower to the geometric mean of the two averaged signal powers, over an integration time interval T. The crosspower and signal-power averages are computed after the two input signals have been bandpass filtered (bandwidth B Hz) and basebanded [4]. Thus the computed ratio is a measure of the normalized correlation envelope of the two signals and constitutes the sample statistic for the NCE estimator. The sample statistic for the MSC estimator is simply the square of the sample statistic for the NCE estimator. In practice, both estimators employ the sectionalized Fourier transform to accomplish the operations of bandpass filtering, basebanding, and signal sampling [4]. As a consequence, complex numbers are involved in the processing, and only the magnitude of the resulting ratio is used in the sample statistics. (This is the reason for the terminology "magnitude-squared" in the case of the MSC estimator, and "magnitude coherence" as the NCE estimator is sometimes called.) Details of these estimators may be found in Ref. 4.

Expected Value of the Sample Statistic

Both the NCE estimator and the MSC estimator are biased estimators. Letting $\hat{\gamma}$ designate the sample statistic for the NCE estimator, its expected or mean value may therefore be written as

$$\langle \hat{\gamma} \rangle = \gamma + \beta_1, \tag{8a}$$

where the bias term β_1 is a function of both γ^2 and the processor time-bandwidth product BT. The square of the mean is simply

$$\langle \hat{\gamma} \rangle^2 = \gamma^2 + \beta_1(2\gamma + \beta_1). \tag{8b}$$

The sample statistic for the MSC estimator is the square of the sample statistic for the NCE estimator or $\hat{\gamma}^2$. The expected value for this estimator is

$$\langle \hat{\gamma}^2 \rangle = \gamma^2 + \beta, \tag{8c}$$

where β represents the bias of this estimator. Since, however, the expected value of the MSC estimator is the second moment of the NCE statistic, it is a simple matter to show that Eq. (8b) may be written as

$$\langle \hat{\gamma} \rangle^2 = \gamma^2 + \beta - \sigma_{\hat{\gamma}}^2, \tag{8d}$$

where $\sigma_{\hat{\gamma}}^2$ is the variance of the NCE statistic. A generalized form for Eqs. (8c) and (8d) may therefore be written as $\gamma^2 + g(\gamma^2; BT)$, where $g(\gamma^2; BT)$ is equal to β in the case of the MSC estimator or $\beta - \sigma_{\hat{\gamma}}^2$ in the case of the NCE estimator. Since β is always positive, $g(\gamma^2; BT)$ will be smaller for the NCE estimator.

4

False-Alarm Probability

Although the probability density functions for the two sample statistics are highly complicated in the general case [9], when γ is equal to zero (input signals are uncorrelated) the probability density functions reduce to

$$p_{\hat{\gamma}}(\hat{\gamma}) = 2(M-1)\hat{\gamma}(1 - \hat{\gamma}^2)^{M-2}, \tag{9a}$$

and

$$p_{\hat{\gamma}^2}(\hat{\gamma}^2) = (M-1)(1 - \hat{\gamma}^2)^{M-2}, \tag{9b}$$

where $M = BT + 1$ is the number of degrees of freedom of the estimator [10]. In either case, the probability that the sample statistic exceeds a threshold level γ_o (producing a false target or alarm) is

$$P_{F.T.} = \int_{\gamma_o^2}^{\infty} p_{\hat{\gamma}^2}(\hat{\gamma}^2)d\hat{\gamma}^2 = \int_{\gamma_o}^{\infty} p_{\hat{\gamma}}(\hat{\gamma}) d\hat{\gamma}$$

$$= (1 - \gamma_o^2)^{BT} \tag{9c}$$

or

$$\gamma_o^2 = 1 - P_{F.T.}^{\frac{1}{BT}}. \tag{9d}$$

THE DETECTION PROBLEM AND SOLUTION OUTLINE

Detection Criterion

Equating the expected value of the coherence estimator to the threshold level for a given probability of false alarm provides a reasonable criterion for target detection. Thus, from Eqs. (8) and (9)

$$\gamma^2 + g(\gamma^2;BT) = \gamma_o^2 \tag{10a}$$

is to be solved for the input signal-to-noise power spectral density ratio r_o as a function of the false-alarm probability $P_{F.T.}$, the processor parameter BT, and the signal parameter ρ. Unfortunately, a straightforward solution to Eq. (10a) is impractical due to the complexity of the bias term $g(\gamma^2;BT)$. On the other hand, for false-slarm probabilities of interest, the influence of the bias term will be to cause only a second-order effect on the solution to the equation. This allows a novel approach to the solution to be taken.

To begin, it may be observed that the influence of the bias term is to reduce the value of γ^2 required for the left-hand side of Eq. (10a) to equal γ_o^2. It therefore proves convenient to let

$$\gamma^2 = \gamma_o^2 - g(\gamma^2;BT) = 1 - P^{\frac{1}{BT}}, \tag{10b}$$

5

where P is some probability greater than $P_{F.T.}$ that is dependent on $P_{F.T.}$, BT, and the bias function $g(\gamma^2;BT)$. The procedure is first to solve the detection criterion in terms of the interim probability P, and then to determine the relationship between the probability parameters P and $P_{F.T.}$ as a function of the processor parameter BT. It turns out that this will involve only minor variations in the ordinate and abscissa scales of the original solution. This approach is equivalent to first solving the problem by ignoring the bias of the estimator, and then demonstrating the changes in the solution required to accommodate the influence of the bias on the resulting solution.

Relationship Between $P(x;P_{F.T.})$ and $P_{F.T.}$

From Eqs. (9d) and (10b) the relationship between the probability function P and the false-alarm probability $P_{F.T.}$ is

$$P_{F.T.}^{\frac{1}{BT}} = P^{\frac{1}{BT}} \left[1 - P^{-\frac{1}{BT}} g\left(1 - P^{\frac{1}{BT}};BT \right) \right] \tag{11a}$$

or

$$\log P_{F.T.} = \log P + BT \log \left[1 - P^{-\frac{1}{BT}} g\left(1 - P^{\frac{1}{BT}};BT \right) \right]. \tag{11b}$$

Letting

$$x = BT/(-\log P), \tag{11c}$$

and noting that

$$P^{\frac{1}{BT}} \equiv \left(0.1 \right)^{\frac{1}{x}}, \tag{11d}$$

relation (11b) becomes

$$\log P_{F.T.} = \log P \left\{ 1 - x \log \left[1 - Z(x;\log P) \right] \right\}, \tag{11e}$$

where

$$Z(x;\log P) = 10^{\frac{1}{x}} g\left\{ 1 - \left(0.1 \right)^{\frac{1}{x}}; -x \log P \right\}. \tag{11f}$$

Although quite complicated, it is possible to solve the implicit function in the variable $\log P$, as a function of x and $\log P_{F.T.}$ (see the appendix).

DETECTION PERFORMANCE RELATIONS

General Solution of Detection Performance

From Eqs. (4) and (10b) the criterion for detection in terms of the input signal-to-noise ratios becomes

$$\gamma^2 = \frac{r^2}{(1 + r^2)(\rho^2 + r^2)} \geq 1 - P^{\frac{1}{BT}} \tag{12a}$$

or

$$r^4 - \left(P^{-\frac{1}{BT}} - 1\right)\left[\left(1 - \rho^2\right)r^2 + \rho^2\right] \geqslant 0. \tag{12b}$$

This is a simple quadratic inequality in r^2 and can readily be solved. Letting $r_o^2 = Br^2$ represent the input signal-to-noise power spectral density ratio, the general detection solution becomes

$$\frac{r_o^2 T}{(-\log P)} = r^2 x$$

$$\geqslant a(\rho)xQ(x)\left[1 + \sqrt{1 + b(\rho)/Q(x)}\right], \tag{12c}$$

where

r_o^2 is the signal-to-noise power spectral density ratio,

r^2 is the signal-to-noise power ratio in the bandwidth B,

T is the processor integration time in seconds,

$a(\rho) = (1 + \rho^2)/2,$

$b(\rho) = \left[2\rho/(1 + \rho^2)\right]^2,$

$x = BT/(-\log P),$

and

$$Q(x) = P^{-\frac{1}{BT}} - 1 \equiv 10^{\frac{1}{x}} - 1.$$

For convenience in modifying the ordinate and abscissa scales to accommodate the effects of the processor bias, given in Eq. (10b), a bias-correcting function $R(x;P_{F.T.})$ is defined as

$$R(x;P_{F.T.}) = \log P_{F.T.}/\log P. \tag{13a}$$

Thus the abscissa scale may be expressed as

$$x = R(x;P_{F.T.})BT/(-\log P_{F.T.}). \tag{13b}$$

Figure 1 shows the family of curves represented by Eq. (12c); the two axes are expressed in terms of the bias-correcting function $R(x;P_{F.T.})$. The derivation of this function for both the NCE and the MSC estimators is given in the appendix. Figures 2 and 3 show families of curves for the function and ten times its logarithm. These curves may be used to determine specific numeric values along the two scales shown in Fig. 1. (An example providing the BT values along the abscissa for $P_{F.T.}$ equal to 10^{-4}, when using the NCE estimator, is given at the top of Fig. 1.) It may be noticed that the influence of the bias on the family of curves (Fig. 1) is to shift the curves to the left and downward (relative to the scales when R is assumed equal to one), with the shift being larger at the higher values of the abscissa scale. This shift in the curves decreases with decreasing false-alarm probability and is relatively small for false-alarm probabilities less than about 10^{-3}. It may also be noted that the shift of both scales for the MSC estimator is approximately twice that for the NCE estimator (for a given value of x and $P_{F.T.}$).

7

The family of curves (Fig. 1) illustrates that there is a defined minimum, or optimum value of BT (noted by the small circles and joined with a dashed curve), except when $\rho = 0$ ($-\infty$ dB). Thus, when the target signal bandwidth W is less than the indicated minimum value for BT divided by the integration time T, optimum detection performance is achieved by overcontainment of the target signal for a given false-alarm probability. It may also be observed that the gradient of detection sensitivity (in dB) is rather moderate in the neighborhood of the optimum BT. This means that one could employ a value BT which is 4 times (or more) the optimum value without suffering a severe penalty in detection sensitivity. These results are in agreement with those of LaPointe in his study on the effects of signal overcontainment on cross-correlation detection performance [7].
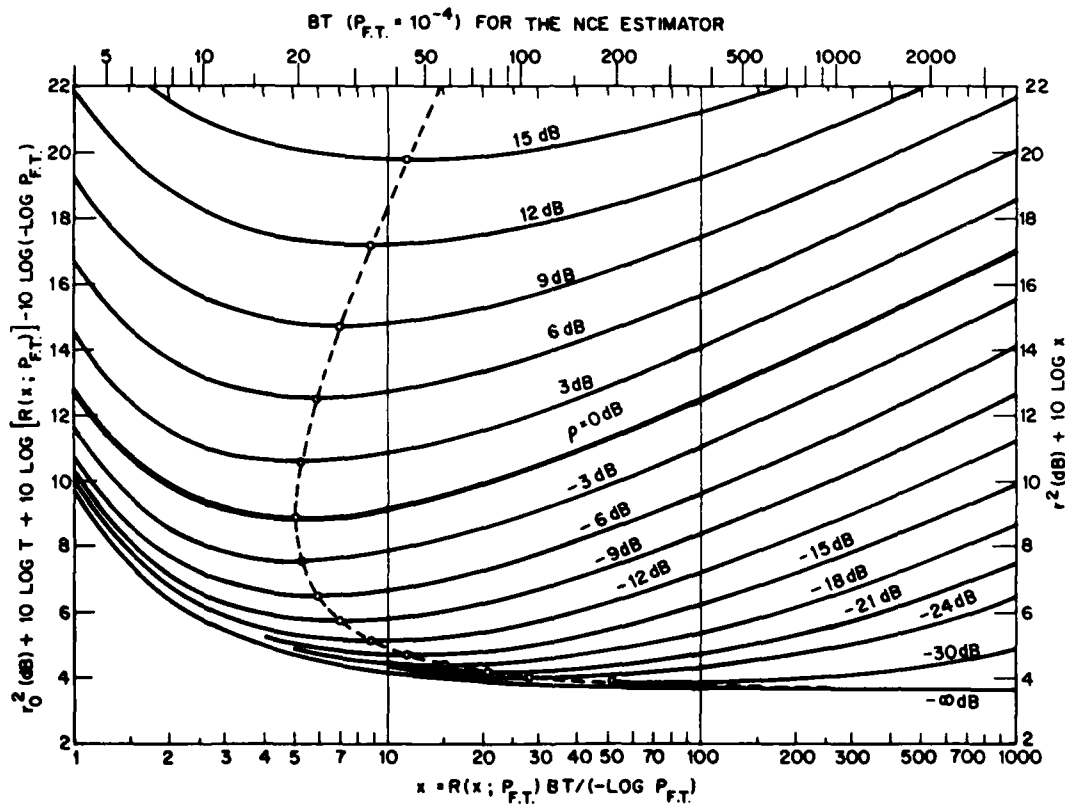

Fig. 1 — Detection performance characteristics for normalized coherence estimators as a function of the signal and processor parameters. The bias correcting function $R(x; P_{F.T.})$ and 10 times its logarithm, for the NCE and MSC estimators, are displayed in Figs. 2 and 3. (The abscissa scale, displayed at the top of the graph, is BT for the NCE estimator when the false-alarm probability is 10^{-4}.) The variable r_o^2 is the input signal-to-noise power spectral density ratio, and r^2 is the in-band signal-to-noise power ratio. The parameter ρ^2 is the ratio of the two input signal-to-noise power ratios. The dashed curve is the locus of detection minima.

Detection Performance in Terms of the Mean Signal-to-Noise
    Ratio of the Two Input Channels

The family of curves shown in Fig. 1 defines the detection performance of the correlation estimator in terms of the signal-to-noise ratio on one of the two signal inputs. Since any excess of signal-to-noise ratio in one of the two channels can partially offset a depletion of signal-to-noise ratio in the second channel, it is interesting to study the degree to which an excess of signal-to-noise ratio in the one channel proves advantageous in target detection. The standard for comparison is that where the two input signal-to-noise ratios are equal ($\rho = 1$ or 0 dB).

The measure of relevance is the geometric mean of the two input signal-to-noise ratios, or the arithmetic mean of the signal-to-noise ratios when expressed in decibels. For $r(x;\rho)$ and ρ expressed in decibels, the arithmetic mean signal-to-noise ratio of the two input channels, expressed in decibels, is

$$r_m(x;\rho) = [r(x;\rho) + r(x;-\rho)]/2$$

$$= r(x;\rho) - \rho/2.$$

(14)

The family of curves in Fig. 1 has been recomputed in terms of the mean input signal-to-noise ratio and is displayed in Fig. 4. These curves demonstrate that when the two input signal-to-noise ratios are unequal, more total signal power (or energy) is required for detection than when the two input signal-to-noise ratios are equal. The increase in signal power is less at the higher values of x (large BT), but becomes increasingly larger as the signal-to-noise ratio imbalance (absolute value of ρ) becomes larger. It is evident that any signal-to-noise ratio excess (amount greater than that required for $\rho = 0$ dB) in the one input channel is partially offset by a decrease in the signal-to-noise ratio of the second channel (required for detection). This utility of the signal-to-noise ratio excess (in the second channel) is explicitly plotted in Fig. 5 as a function of the signal-to-noise ratio excess and the value of x. These curves demonstrate that initially the trade-off in signal-to-noise ratio is nearly one-to-one. That is, the detection criterion can be based on the mean signal-to-noise ratio of the two input channels, provided the signal-to-noise ratio imbalance is sufficiently small. However, when the imbalance in the input signal-to-noise ratios becomes large, the utility of the signal excess in the one channel decreases and eventually saturates (see Fig. 5). At this point, the correlation processor is functioning as a matched filter or replica correlator, and no further improvement in processing gain can be expected.

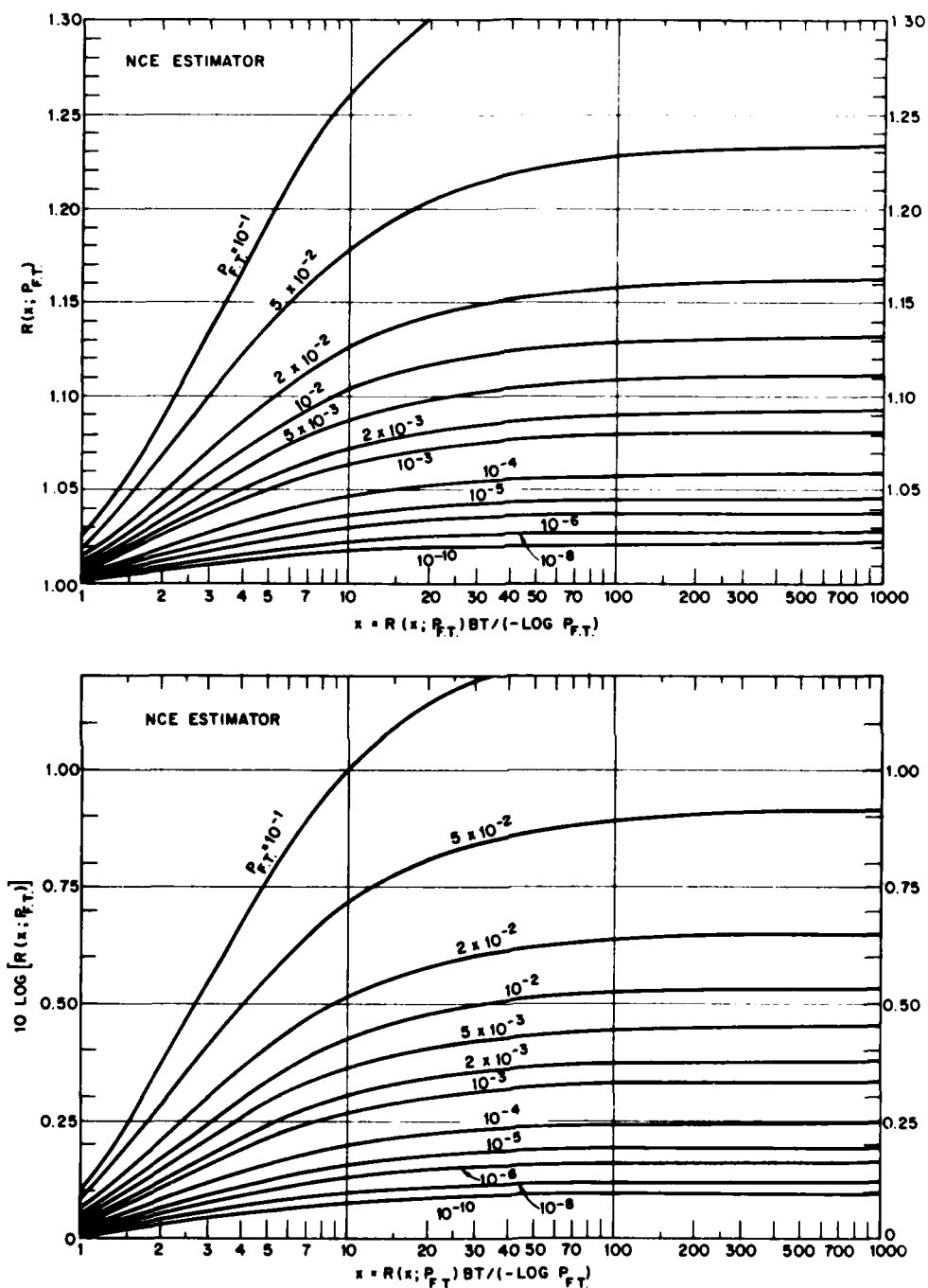Fig. 2 — Curves of the bias-correcting function $R(x; P_{F.T.})$ and 10 times its logarithm for the NCE estimator. These curves may be used to convert the scales in Fig. 1 to relevant numeric values. (See the appendix for derivation of the curves.)
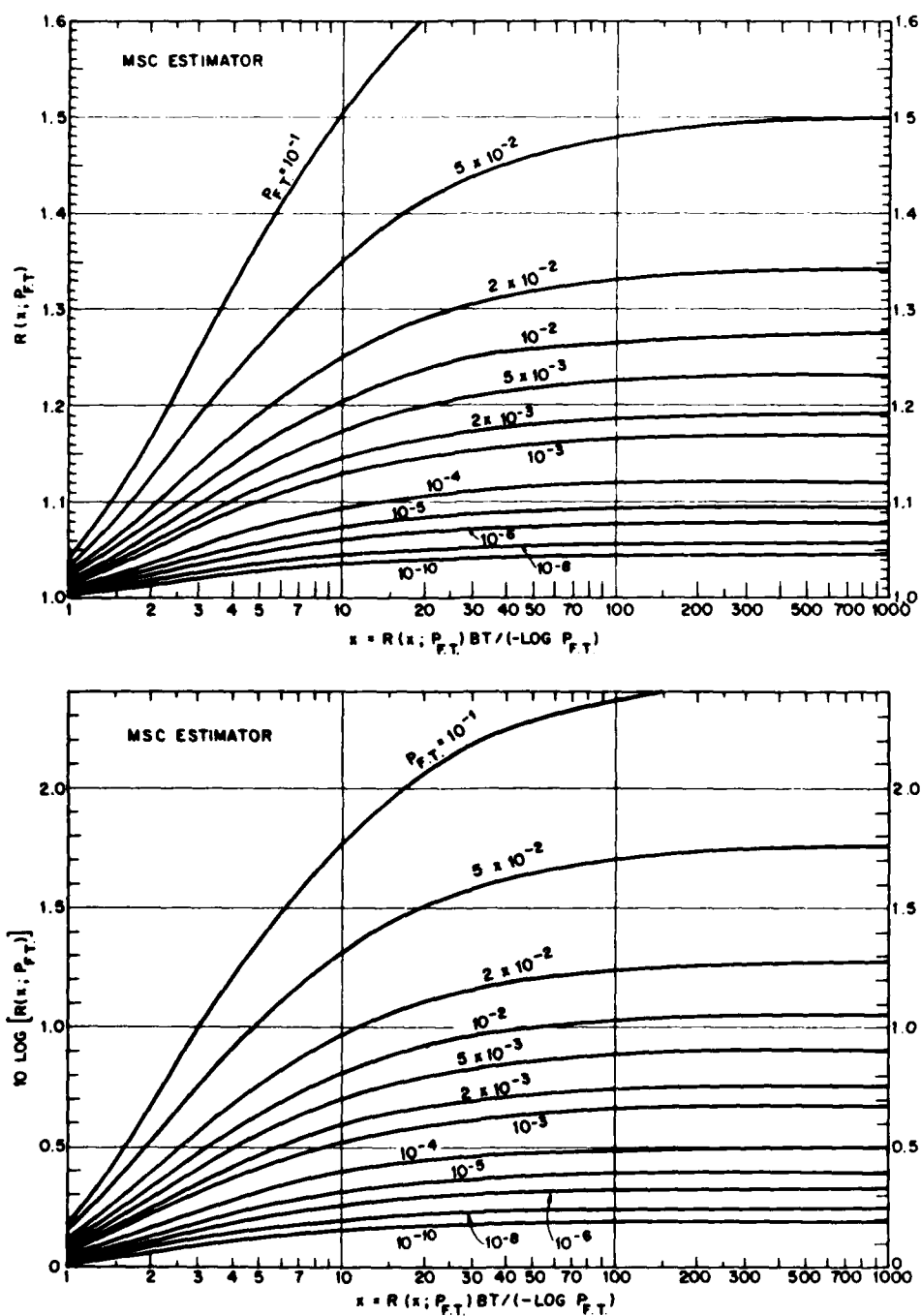
Fig. 3 — Curves of the bias-correcting function $R(x; P_{F.T})$ and 10 times its logarithm for the MSC estimator. These curves may be used to convert the scales in Fig. 1 to relevant numeric values. (See the appendix for derivation of the curves.)
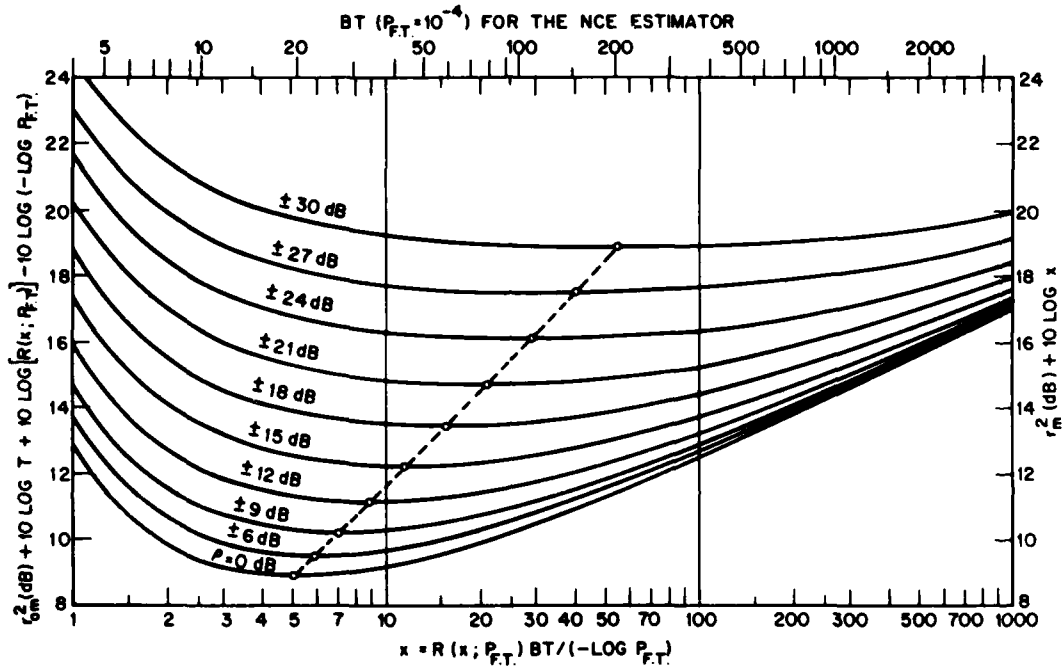
Fig. 4 — Detection performance characteristics for normalized coherence estimators in terms of the geometric mean of the two input signal-to-noise power ratios. The bias-correcting function $R(x; P_{F.T.})$ and 10 times its logarithm, for the NCE and MSC estimators, are displayed in Figs. 2 and 3. (The abscissa scale, displayed at the top of the graph, is BT for the NCE estimator when the false-alarm probability is 10^{-4}.) The variable r_{om}^2 is the geometric mean of the two input signal-to-noise power spectral density ratios, and r_m^2 is the geometric mean of the two in-band signal-to-noise power ratios. The parameter ρ^2 is the ratio of the two input signal-to-noise power ratios. The dashed curve is the locus of detection minima.
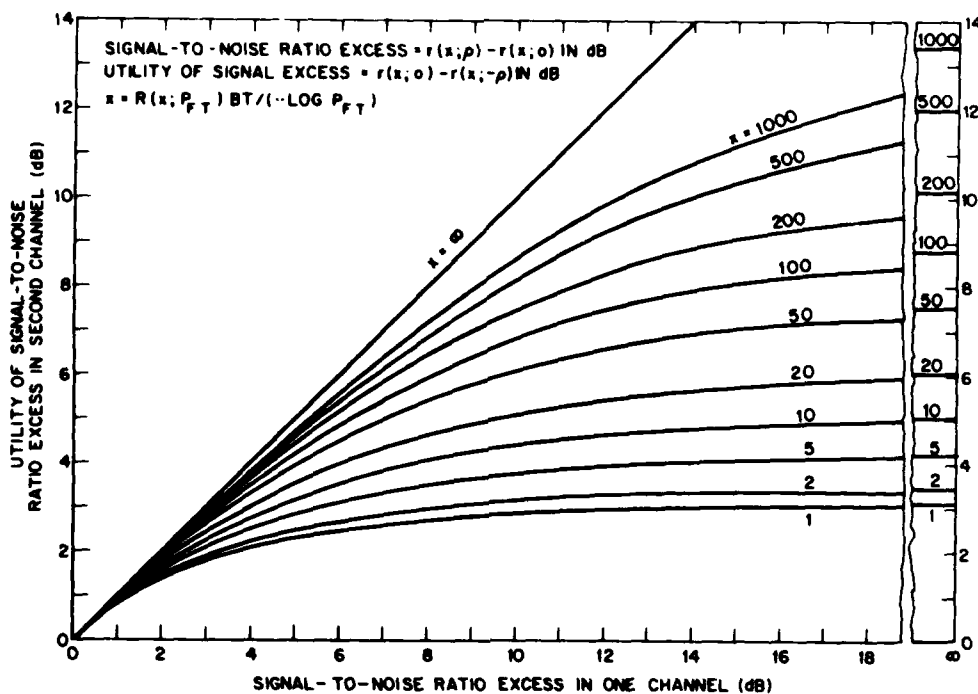
Fig. 5 — Curves illustrating the utility of an excess of signal-to-noise ratio in one channel in lowering the signal-to-noise ratio, required for detection, of the second channel. The dB measure, in either case, is referenced to that required for detection when the signal-to-noise ratios of both channels are equal ($\rho = 0$ dB).

Detection Performance Topology

Figure 6 displays another way of illustrating the detection performance of the coherence estimator. Here the topological contours give the performance degradation (in 0.5 dB steps) relative to the optimum point in the x, ρ plane (located at $x = 5.04$, $\rho = 0$ dB). (These contours do not include the bias function term $10 \log R$ given in Figs. 2 or 3. However, for most false-alarm probabilities of interest, this bias function term does not significantly change the contours.) The dashed curve represents the locus of points of minimum coherence degradation along the ρ axis. Since $W \leqslant B$, the illustrated topology is valid only over the area where $WT \leqslant BT$. For a given W and T, a horizontal line should be drawn at the appropriate ordinate value on Fig. 6, and only values above this line are valid. Below this line, the degradation would be more severe than that shown due to the loss in target signal energy resulting from the decreased processor bandwidth.

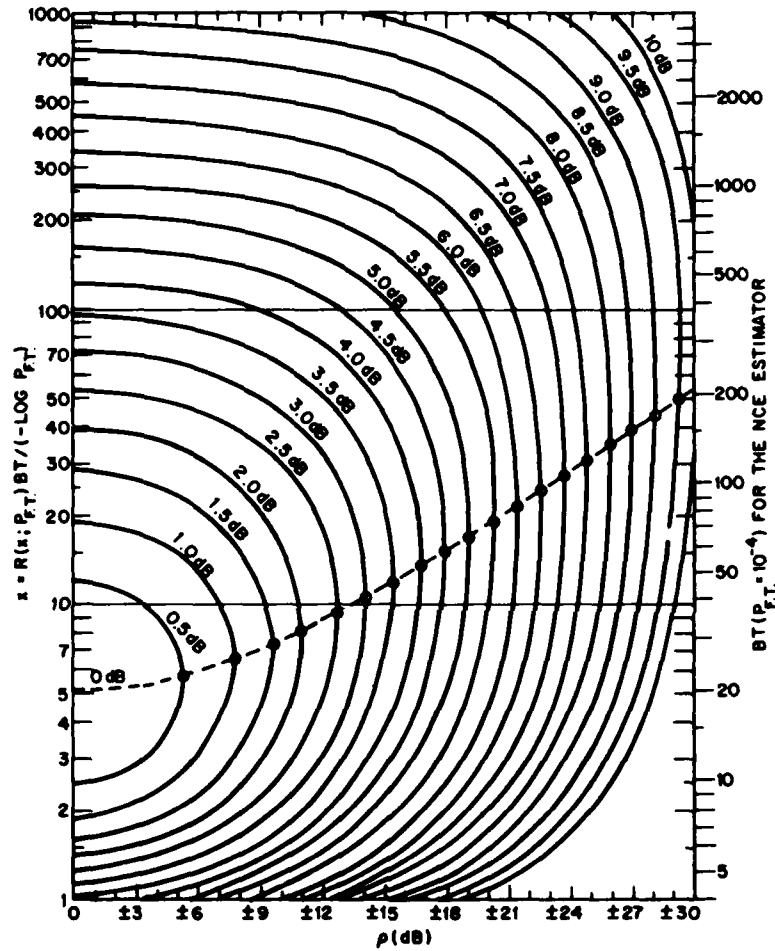Fig. 6 — Topological contours of peak-coherence degradation, relative to the optimum performance, over the x, ρ plane. The contours do not include the bias-function term $10 \log R$. However, for most false-alarm probabilities of interest, this bias-function term will not significantly change the contours. The dashed curve represents the locus of points of minimum coherence degradation along the ρ axis.

OPTIMUM DESIGN CONSIDERATIONS

Parameter Selection Criteria

In practical applications, the user of a correlation processor is interested in achieving detection at the lowest total input signal power consistent with other considerations outside of his control. A study of Fig. 4 reveals that the ordinate scale is dependent on the integration time T, the false-alarm probability $P_{F.T.}$, the bias-correcting function $R(x; P_{F.T.})$, and the power spectral density r_o^2. The influence of the bias-correcting function is relatively insignificant. And, although the detection sensitivity can be enhanced by operating at a high false-alarm probability, the choice here is limited by the number of false alarms that one is willing to accept in a given application. A more important consideration is the integration time of the processor. One may readily observe that each doubling of the integration time will lower the ordinate scale by 3 dB. This rate is sufficient to offset the maximum 1.5 dB per octave rise in the curves (Figs. 1 and 4) which may result from the increased value of BT. Consequently, the system designer should use as long an integration time as is practical from other considerations. For many applications, however, the maximum useful integration time is limited by factors outside of the control of the system designer. In this situation, one should compute the value for WT and draw a lower boundary line at the appropriate x value on Figs. 1, 4, and 5. When this boundary is above the minimum value of the relevant curve it is the optimum operating point of the processor. That is, the processor bandwidth B should be set equal to the signal bandwidth W. On the other hand, if the lower boundary is below the minimum value of the curve, optimum detection performance is achieved when the processor bandwidth B is increased to the point where BT on the appropriate curve (for the parameter ρ) indicates a minimum.

Detection Performance Sensitivity to Parameter Selection

To select the processor bandwidth B for optimum detection, in an absolute sense, requires knowledge of the input signal parameters W and ρ. Unfortunately, for many applications the signal bandwidth W is generally not known precisely. And the ratio of the input signal-to-noise ratios is an uncontrollable parameter which can vary over wide limits. Under these circumstances, the sensitivity of the detection performance to variations in the parameter BT, about the optimum value for a given ρ, becomes important. In theory, it is possible to choose a value of BT which optimizes the detection performance in a statistical sense. However, to carry out the analysis requires *a priori* knowledge of the relevant statistics for ρ and W over the ensemble of values (for these parameters) to be expected in a given application. Unfortunately, these statistics are generally not known with precision, which increases the importance of the detection sensitivity to the selection of an appropriate value for the parameter BT.

To demonstrate the sensitivity of detection performance to the selection of BT, the data in Fig. 6 have been redrawn to reflect the degradation in detection performance resulting from choosing suboptimal values of BT for a given value of ρ. Figure 7 illustrates the resulting curves. The curve entitled *Locus of Detection Minima* reflects the optimum value of BT as a function of the signal parameter ρ. The dashed curves (on either side of this curve) reflect values of BT which result in the given performance degradation from that which is optimum. These curves demonstrate that the detection performance is not highly sensitive to the choice of the parameter BT, and the sensitivity decreases as $|\rho|$ becomes larger. For example, the variation in the selection of BT at $\rho = 0$ dB can be 4.8 to 1 and at $\rho = \pm18$ dB can be 12.5 to 1, without suffering a loss in detection performance greater than 0.5 dB. This insensitivity to detection performance is also evident in a study of the curves shown in Figs. 1, 4, and 6 (from which the curves in Fig. 7 are derived).
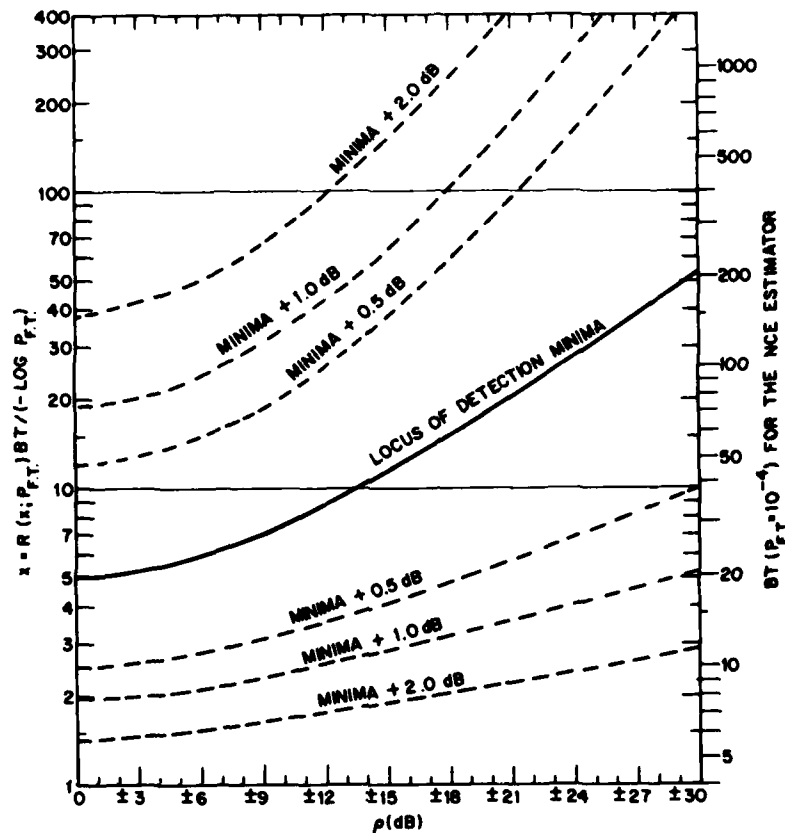
Fig. 7 — Curves reflecting the sensitivity in peak coherence performance to the deviation of the processor parameter BT from its optimum value. The curves are applicable only for processor bandwidths B equal to or greater than the signal bandwidth.

To use the curves (Fig. 7), one should first determine the maximum value of signal bandwidth W that can reasonably be expected. A horizontal line should then be drawn at the value WT for the chosen $P_{F.T.}$ and estimator to be employed. This horizontal line, in conjunction with the Locus of Detection Minima, serves as a lower bound in the selection of the processor parameter BT. One may then estimate the range of values for the parameter ρ over which detection may be expected in the given application. The optimum selection for BT lies somewhere in the neighborhood of the lower bound over the indicated range of ρ. The precise selection of BT depends on the probability densities adjudged for the statistical variables ρ and W. In any event, it can be observed that considerable latitude is available in the selection of BT without seriously degrading the detection performance of the coherence estimator. As an example, if WT occurs at $x = 10$ (40 for the NCE estimator operating at $P_{F.T.} = 10^{-4}$) or below, and ρ can range over ± 30 dB, then BT can be between 40 and 72 (for the indicated estimator) without serious performance degradation.

Some caution is warranted in the application of the above procedures. Recall that the preceding analysis is based on a flat noise or interference signal spectrum over the spectral range in which B is varied. This is a reasonable assumption for many applications of narrowband detection processors. However, it does not consider the existence of narrowband interfering signals which can

16

radically degrade the input signal-to-noise (interference) ratio when they fall within the processor bandwidth B. Consequently, when there is a large number of narrowband interfering signals distributed in the spectral region of the anticipated target signal, this fact would favor a lower-than-otherwise choice for BT (to reduce the probability of a strong interfering signal from falling within the processor bandwidth B). The selection of processor design parameters, which are optimum in a true operational sense, does require a fair amount of human experience and judgment in most practical applications.

CONCLUSIONS

1. Optimum performance of passive coherence estimators is not necessarily realized by matching the processor bandwidth to the bandwidth of the target signal, even when the target signal bandwidth is known *a priori*. In many practical applications, particularly when the time-bandwidth product of the target signal is severely limited, detection performance is enhanced by overcontainment of the target signal within the processor bandwidth.

2. The optimum processor bandwidth and the resulting detection performance are functions of the correlator integration time, the ratio of the two input signal-to-noise ratios, and the false-alarm probability threshold. For a fixed integration time and false-alarm probability, the optimum processor bandwidth increases as the ratio of the two input signal-to-noise ratios deviates from 1 (0 dB). However, the degradation in detection performance to deviations of the processor bandwidth from its optimum value becomes decreasingly less (see Fig. 7).

3. For a given processor time-bandwidth product and false-alarm probability, the minimum total signal power required for detection is realized when two input signal-to-noise ratios are equal (see Fig. 4). As the ratio of the two input signal-to-noise ratios deviates from 1 (0 dB), greater total input signal power is required for detection. However, the required power increase becomes less as the time-bandwidth product of the process becomes greater. The efficiency of the trade-off in the two input signal-to-noise ratios, as a function of the processor time-bandwidth product and the signal-to-noise ratio excess in the one input channel, is given in Fig. 5.

4. The relations developed in this analysis are based on a uniform noise or interference spectrum over the range of processor bandwidths employed. Therefore, caution is required when there exists a large number of narrowband interfering signals which are likely to fall within the selected processor bandwidth. This particular situation would favor a lower-than-otherwise choice for the processor bandwidth to reduce the probability of a strong interfering signal from degrading the detection sensitivity of the processor.

ACKNOWLEDGMENTS

REFERENCES

1. G. C. Carter, "Estimation of the Magnitude-Squared Coherence Function (Spectrum)," Naval Underwater Systems Center Report No. TR4343, May 1972.

2. J. J. Gosselin, "Comparative Study of Two-Sensor Magnitude-Squared Coherence and Single Sensor Square-Law Receiver Operating Characteristics," *Proc. IEEE/ICASSP-77*, 311-314, 1977.

3. R. D. Trueblood and D. L. Alspach, "Multiple Coherence as a Test Statistic," NOSC Report TR-265, July 1978.

4. A. A. Gerlach, "High-Speed Coherence Processing Using the Sectionalized Fourier Transform," *IEEE Trans. on Acoustics, Speech, and Signal Processing* ASSP-30(2), 189-205, Apr. 1982.

5. A. A. Gerlach, *Theory and Applications of Statistical Wave-Period Processing*, Gordon and Breach, Science Publishers Inc., New York, 1970, pp. 117-129.

6. J. R. LaPointe, Jr., "Ambiguity Surface Statistics and Overcontainment," Analytical Technology Applications Corporation Report SV8007-1, Sep. 1981.

7. J. R. LaPointe, Jr., "The Impact of Overcontainment on Cross-Correlation Detection Performance," *Proc. IEEE:IC*ASSP-82, Paris, France, May 1982.

8. A. A. Gerlach, op cit [5], Eq. (3.11-27).

9. N. R. Goodman, "On the Joint Estimation of the Spectra, Cospectrum, and Quadrature Spectrum of a Two-Dimensional Stationary Gaussian Process," *Science Paper No. 10, Engineering Statistics Laboratory*, New York University; Mar. 1957.

10. A. A. Gerlach, op cit [4], Eq. (31b).

Appendix

BIAS-CORRECTING FUNCTION $R(x;P_{F.T.})$

The relationship between the interim probability P and the false-alarm probability $P_{F.T.}$ is given in Eq. (11) as

$$\log P_{F.T.} = \log P \left\{ 1 - x \log \left[1 - Z(x; \log P) \right] \right\}, \tag{A-1a}$$

where

$$Z(x; \log P) = 10^{\frac{1}{x}} g \left\{ 1 - \left(0.1\right)^{\frac{1}{x}}; -x \log P \right\}, \tag{A-1b}$$

and where $g(\gamma^2; BT) = \beta$ in the case of the MSC estimator or $g(\gamma^2; BT) = \beta - \sigma_\gamma^2$ in the case of the NCE estimator. It is desired to solve the implicit function (A-1a) for $P(x; P_{F.T.})$ and compute the bias-correcting function

$$R(x; P_{F.T.}) = \log P_{F.T.} / \log \left[P(x; P_{F.T.}) \right]. \tag{A-1c}$$

This requires explicit knowledge of the bias function β and the variance σ_γ^2.

The Function $R(x; P_{F.T.})$ for the MSC Estimator

Both the bias and the variance functions of concern involve rather complicated forms of the generalized hypergeometric function. However, Nuttall and Carter have derived rather precise approximations to these functions which will be quite suitable for the purpose of this report [A1]. The details of the approximations and their precision may be obtained from Ref. A1.

Expressed in the terminology of this report, the approximation for the bias function β becomes

$$\beta(\gamma^2; BT) = \frac{(1 - \gamma^2)^2}{BT + 1} \left(1 + 2 \frac{\gamma^2}{BT + 1} \right). \tag{A-2a}$$

Letting $p = -\log P = \log (1/P)$, the function $Z(x; \log P)$ for the MSC estimator is, from Eq. (A-1b),

$$Z(x; \log P) = \frac{(0.1)^{\frac{1}{x}}}{px + 1} \left[1 + 2 \frac{1 - (0.1)^{\frac{1}{x}}}{px + 1} \right]. \tag{A-2b}$$

By use of this function in Eq. (A-1a), the implicit function has been solved on the computer for values of $P_{F.T.}$ ranging from 10^{-1} to 10^{-10}. Graphs of the function $R(x; P_{F.T.})$ and 10 times its logarithm, for the MSC estimator, are plotted in Fig. 3.

19

When x is very large, $Z(x;\log P)$ approximates $1/px$, and it is easy to show that

$$\lim_{x \to \infty} R(x;\log P) = \left[1 + \frac{\log e}{\log P_{F.T.}} \right]^{-1}. \tag{A-2c}$$

The Function $R(x; P_{F.T.})$ for the NCE Estimator

Expressed in the terminology of this report, the approximation for the variance $\sigma_{\hat{\gamma}}^2$ provided by Nuttall and Carter [A1] becomes

$$\sigma_{\hat{\gamma}}^2 = \frac{(1-\gamma^2)^2}{2(BT-1)} \left[1 - 3\frac{1-\gamma^2}{BT+1} - \frac{(1-\gamma^2)^2}{(BT+1)^2} \times \frac{A}{1+B\gamma^2+C\gamma^4} \right], \tag{A-3a}$$

where

$$A = 0.571(BT)^2 - 0.608BT - 1.939$$

$$B = 0.752BT - 2.508$$

$$C = 0.221(BT)^2 - 1.218BT - 1.439.$$

Again lettering $p = -\log P = \log(1/P)$, with a little algebraic manipulation the function $Z(x;\log P)$ may be shown to be

$$Z(x;\log P) = \frac{(0.1)^{\frac{1}{x}}}{2(px+1)} \left\{ 1 + \frac{2-(0.1)^{\frac{1}{x}}}{px-1} - \frac{8}{p^2x^2-1} \left[1 - (0.1)^{\frac{1}{x}} \right. \right.$$

$$\left. \left. - \frac{(0.1)^{\frac{2}{x}} f_1(px)}{f_2(px) - (0.1)^{\frac{1}{x}} f_3(px) + (0.1)^{\frac{2}{x}} f_4(px)} \right] \right\}, \tag{A-3b}$$

where

$$f_1(px) = 0.071375(px)^2 - 0.076px - 0.242375$$

$$f_2(px) = 0.221(px)^2 - 0.466px - 2.947$$

$$f_3(px) = 0.442(px)^2 - 1.684px - 5.386$$

$$f_4(px) = 0.221(px)^2 - 1.218px - 1.439.$$

By use of this function in Eq. (A-1a), the implicit function has been solved on the computer for values of $P_{F.T.}$ ranging from 10^{-1} to 10^{-10}. Graphs of the function $R(x;P_{F.T.})$ and 10 times its logarithm, for the NCE estimator, are plotted in Fig. 2.

The solution of $Z(x; P_{F.T.})$ when x is very large is not simple in the case of the NCE estimator. However, by employing L'Hospital's Rule it can be shown that for large x

$$Z(x; \log P) \approx \frac{1}{2px} \left[1 + \frac{0.571}{1.1717p^2 + 1.7315p + 1} \right]. \tag{A-3c}$$

Consequently, for p sufficiently large ($P_{F.T.}$ sufficiently small) a suitable approximation for the limit of $R(x; P_{F.T.})$ as x becomes very large is

$$\lim_{x \to \infty} R(x; P_{F.T.}) \approx \left[1 + \frac{\log e}{2 \log P_{F.T.}} \right]^{-1} \tag{A-3d}$$

A study of the curves in Figs. 1 and 2 reveals that the value of $R(x; P_{F.T.})$ for the NCE estimator is approximately equal to one-half times one plus the value of $R(x; P_{F.T.})$ for the MSC estimator, over much of the range of x and $P_{F.T.}$.

Scale Values for $P_{F.T.} = 10^{-4}$

To demonstrate the influence of the bias-correcting function on the scales of the graphs presented in the report, the values of x and $10 \log R(x; P_{F.T.})$ have been computed for a false-alarm probability $P_{F.T.}$ of 10^{-4} and BT ranging from 4 to 3000. Table A-1 gives the results. The first column displays the values of the abscissa x for an ideal unbiased estimator; that is, when $R(x; P_{F.T.}) = 1$. In this case, x is simply equal to BT divided by $\log (1/P_{F.T.})$, and no scale correction is required. The corresponding values of x for the biased estimators may then be compared with those of the ideal estimator to assess the influence of the bias on the scales. Note that the influence of the bias increases with the abscissa variable x out to about $x = 20$, after which it levels off. The overall effect of the bias (relative to the ideal unbiased estimator) is to slightly shift the detection-performance curves in Figs. 1 and 4 to the left and downward. The resulting influence on the scales can generally be ignored for false-alarm probabilities less than about 10^{-4}. Scale markings of BT, for the NCE estimator and $P_{F.T.} = 10^{-4}$, have been included on the detection-performance curves presented in the report.

REFERENCE

A1. A. H. Nuttall and G. C. Carter, "Approximations for Statistics of Coherence Estimators," NUSC Technical Report 5291, Naval Underwater Systems Center, 9 Mar. 1976

Table A-1 — Abscissa Values x and $10 \log [R(x;P_{F.T.})]$, as a Function of BT, for the Coherence Estimators when $P_{F.T.} = 10^{-4}$

BT	Ideal: $R(x;P_{F.T.}) = 1$		NCE Estimator		MSC Estimator	
	x	$10 \log R$	x	$10 \log R$	x	$10 \log R$
4	1.000	0	1.005	0.02	1.012	0.05
5	1.250	0	1.265	0.04	1.275	0.07
6	1.50	0	1.52	0.05	1.54	0.11
7	1.75	0	1.78	0.07	1.81	0.15
8	2.00	0	2.04	0.08	2.08	0.16
9	2.25	0	2.30	0.09	2.34	0.17
10	2.50	0	2.56	0.10	2.62	0.20
15	3.75	0	3.87	0.14	3.99	0.27
20	5.00	0	5.19	0.16	5.38	0.32
30	7.50	0	7.83	0.18	8.16	0.37
40	10.00	0	10.48	0.20	10.96	0.40
50	12.50	0	13.12	0.21	13.74	0.41
60	15.00	0	15.77	0.21	16.54	0.42
70	17.50	0	18.42	0.22	19.34	0.43
80	20.00	0	21.07	0.22	22.15	0.44
90	22.50	0	23.72	0.22	24.95	0.45
100	25.00	0	26.37	0.23	27.75	0.45
150	37.50	0	39.62	0.23	31.74	0.46
200	50.00	0	52.80	0.24	55.60	0.48
300	75.00	0	79.30	0.24	83.80	0.48
400	100.0	0	105.7	0.24	111.9	0.49
500	125.0	0	132.2	0.24	139.9	0.49
600	150.0	0	158.7	0.24	167.9	0.49
700	175.0	0	185.5	0.25	196.0	0.49
800	200.0	0	211.7	0.25	224.0	0.49
900	225.0	0	238.0	0.25	252.0	0.49
1000	250 0	0	264.6	0.25	280.1	0.49
1500	375.0	0	396.9	0.25	420.4	0.50
2000	500.0	0	529.3	0.25	560.6	0.50
3000	750.0	0	794.0	0.25	841.0	0.50

DATE
FILME